

# Elucidation of Two Giants: Challenges to Thick-Shell Synthesis in CdSe/ZnSe and ZnSe/CdS Core/Shell Quantum Dots

Krishna P. Acharya,<sup>†</sup> Hue M. Nguyen,<sup>†</sup> Melissa Paulite,<sup>†</sup> Andrei Piryatinski,<sup>‡</sup> Jun Zhang,<sup>§</sup> Joanna L. Casson,<sup>||</sup> Hongwu Xu,<sup>§</sup> Han Htoon,<sup>†</sup> and Jennifer A. Hollingsworth<sup>\*,†</sup>

<sup>†</sup>Materials Physics and Applications Division: Center for Integrated Nanotechnologies, <sup>‡</sup>Theoretical Division: Physics of Condensed Matter & Complex Systems, <sup>§</sup>Earth & Environmental Science Division: Earth System Observations, <sup>||</sup>Chemistry Division: Physical Chemistry & Applied Spectroscopy, Los Alamos National Laboratory, Los Alamos, New Mexico 87545, United States

## S Supporting Information

**ABSTRACT:** Core/thick-shell giant quantum dots (gQDs) possessing type II electronic structures exhibit suppressed blinking and diminished nonradiative Auger recombination. We investigate CdSe/ZnSe and ZnSe/CdS as potential new gQDs. We show theoretically and experimentally that both can exhibit partial or complete spatial separation of an excited-state electron–hole pair (i.e., type II behavior). However, we reveal that thick-shell growth is challenged by competing processes: alloying and cation exchange. We demonstrate that these can be largely avoided by choice of shelling conditions (e.g., time, temperature, and QD core identity). The resulting CdSe/ZnSe gQDs exhibit unusual single-QD properties, principally emitting from dim gray states but having high two-exciton (biexciton) emission efficiencies, whereas ZnSe/CdS gQDs show characteristic gQD blinking suppression, though only if shelling is accompanied by partial cation exchange.

Semiconductor quantum dots (QDs) are an important class of photoluminescent material whose chemistry, photo-physical properties, and potential applications have been widely elaborated.<sup>1</sup> Interest in QDs has stemmed in large part from the now well-known susceptibility of the semiconductor bandgap to small changes in nanocrystal size.<sup>2</sup> The resulting size-tunable QD absorption and emission energies, along with their characteristic efficient narrow-band emission and broadband absorption, renders them nearly ideal fluorophores for a range of applications from single-particle tracking to efficient lighting.

However, until relatively recently,<sup>3</sup> QDs were limited by seemingly intrinsic processes: fluorescence intermittency, or blinking, and nonradiative Auger recombination (AR). Blinking impacts applications requiring single-QD-level photostability/reliability, e.g., tracking or single-photon sources for quantum information processing, whereas AR quenches emission (at least partially) from complex excitations, i.e. excited states beyond the simple exciton, or electron–hole pair, e.g., charged excitons (extra electron or hole) or multiple excitons. In this way, AR impacts applications in solid-state lighting<sup>4</sup> and lasing,<sup>5</sup> respectively.

Though not necessarily always causally linked,<sup>6</sup> common synthetic solutions were found that addressed both blinking and AR, which entailed modifying the QD to include a thick

shell of a higher-bandgap semiconductor<sup>3a–c</sup> or introducing an alloyed composition at the core/shell interface.<sup>3d</sup> Interestingly, the thick or giant shell approach has to date only been demonstrated for core/shell QDs characterized by a spatially separated exciton.<sup>3a–c</sup> Specifically, excitons in CdSe/CdS giant QDs (gQDs) experience partial spatial separation (quasi-type II electronic structure), with the hole confined to the core and the electronic wave function spreading into the shell.<sup>3a,b</sup> In InP/CdS gQDs,<sup>3c</sup> the electron and hole are fully spatially separated (type II electronic structure) between the shell and core, respectively.

Here, with successful gQD systems as our model, we sought to establish new nonblinking/suppressed-AR thick-shell QDs based on quasi- or fully type II electronic structures. Considering core/shell valence and conduction-band alignments (Figure 1a,c insets), CdSe/ZnSe is a type I structure, whereas ZnSe/CdS is type II. However, the small hole step potential ( $\Delta U_h$ , Figure 1a inset) of the CdSe/ZnSe system suggests that this core/shell may also be characterized by quasi-type II behavior. Indeed, we find that for sufficiently small core sizes, the hole wave function can delocalize into the shell, where the resulting quasi-type II regime is shown in the plot of calculated wave function overlap integrals (Figure 1a). Decreasing overlap integral values in/around this regime stem from reduced electron–hole interactions caused by hole delocalization. This result (localized electron/delocalized hole) is opposite that for CdSe/CdS gQDs (delocalized electron/localized hole).

The clearly staggered band alignment of the ZnSe/CdS system presents a simpler picture for this definitively type II structure. For a wide range of core sizes and shell thicknesses, the electron and hole are localized to different regions of the structure: the hole to the core and the electron to the shell (Figure 1c). The impact of structure on the bandgap of the two systems also differs. In the case of CdSe/ZnSe, core size plays the primary role in determining bandgap energy (Figure 1b); whereas, bandgap for ZnSe/CdS is influenced by both core size and shell thickness (Figure 1d).

Synthesis of the theoretically defined structures is challenged by two further characteristics of these systems. Namely, CdSe/ZnSe is prone to cation-mixing and  $\text{Zn}_x\text{Cd}_{1-x}\text{Se}$  alloy formation; whereas, as we show, ZnSe undergoes rapid cation

Received: January 15, 2015

Published: March 6, 2015



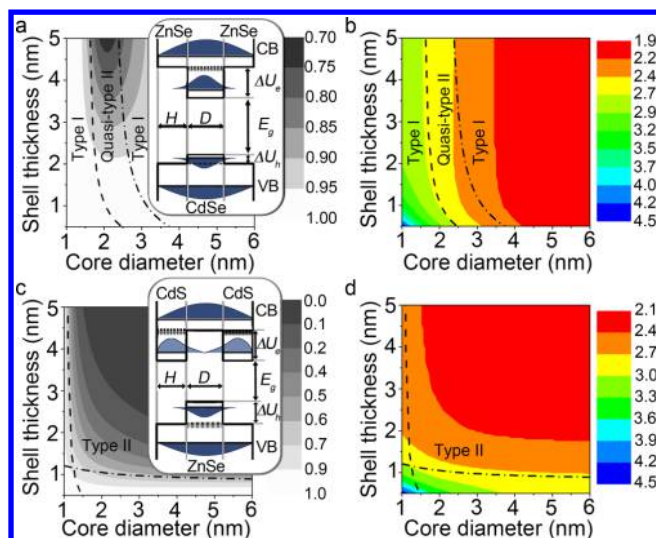


**Figure 1.** Theoretical shell thickness ( $H$ ) and core diameter ( $D$ ) dependencies for (a) CdSe/ZnSe electron-hole overlap integral, (b) CdSe/ZnSe bandgap energy ( $E_g$  in eV), (c) ZnSe/CdS overlap integral, and (d) ZnSe/CdS ( $E_g$  in eV, using effective mass approximation).<sup>3c</sup> Insets in (a and c) depict the band diagram for CdSe/ZnSe and ZnSe/CdS core/shell QDs, respectively (VB, valence band; CB, conduction band;  $\Delta U_h/\Delta U_e$ , hole and electron step potential, respectively). Regions where specific electronic structures are expected to prevail are also indicated.

exchange during CdS shell growth, with Cd replacing Zn to form structures best characterized as ZnSe/CdSe/CdS core/shell/shell QDs. In all instances where we employ separate anion and cation precursors (dual source reactions), we use the successive ionic layer adsorption and reaction (SILAR) method for monolayer-by-monolayer shell addition (Supporting Information)<sup>7</sup> used previously for gQD syntheses.<sup>3a-c,8</sup>

CdSe/ZnSe core/thin-shell QDs have been reported for shell-growth at  $T \leq 200$  °C.<sup>9</sup> However, the core/shell structure is known to give way to homogeneous alloy ( $\text{Zn}_x\text{Cd}_{1-x}\text{Se}$ ) formation at  $T \geq 270$  °C.<sup>10</sup> We find that depending upon synthesis parameters the alloying point temperature can be significantly lower, where a key factor is the annealing time permitted for shell formation (long = 2 h following Zn addition and 1 h following Se addition; short = 10 min between shell-precursor additions).

In Figure 2, we show the evolution of absorption and photoluminescence (PL) spectra as a function of shell thickness and for short or long SILAR anneal times, where the 240 °C reaction temperature is below the previously reported alloying point. Interestingly, although short anneal times afford simple shell growth out to 12 ZnSe monolayers (1 ML  $\approx$  0.33 nm), longer anneal times promote cation mixing and alloy formation. Core/shell growth is evident in the progressive enhancement in absorption at  $<440$  nm (ZnSe bulk bandgap) as a function of increasing number of shell MLs as well as PL shifts to longer wavelengths. Similar trends are observed for CdSe/CdS gQDs.<sup>3a,b</sup> Here, the small shift with shell ML is consistent with our calculations as discussed above.

In contrast, alloy formation is indicated by extensive blue-shifting in absorption and PL (i.e., to an intermediate value between the CdSe bulk bandgap of 1.74 eV/713 nm, and the ZnSe bandgap of 2.82 eV/440 nm, Figure 2c,d). The resulting structure may be a homogeneous alloy or, as observed previously for systems less Zn-rich, compositionally graded

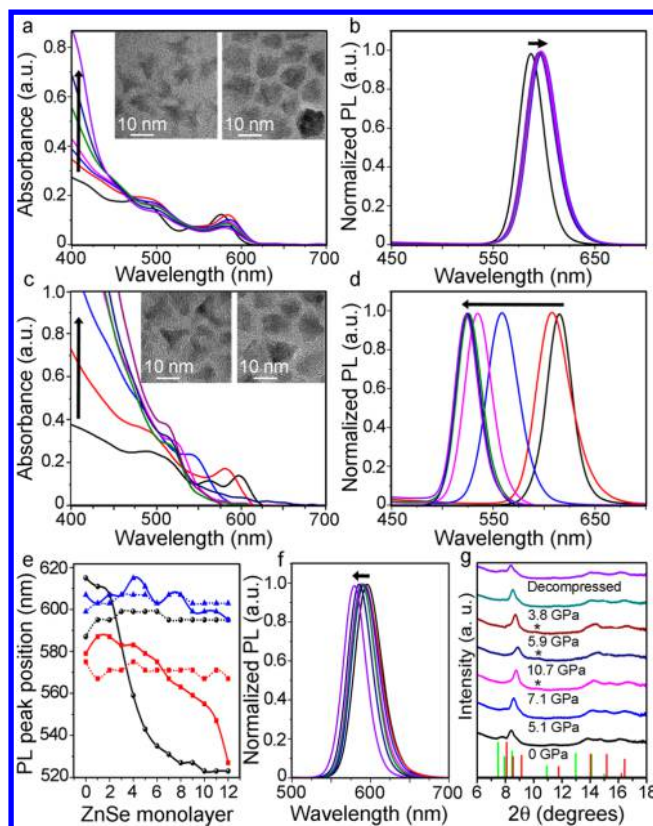


**Figure 2.** (a) Absorption and (b) PL spectra for CdSe core (black trace, zinc blende phase) and after short-cycle SILAR ZnSe shell addition (even MLs 2–12). (c and d) Same for a long-cycle reaction. Insets in a and c: TEM images of 12 ML products from zinc blende (left) and wurtzite (right) cores. (e) PL peak progression with ZnSe-shell ML for different shelling conditions and CdSe cores: short (dashed traces) or long (solid traces) anneal times using zinc blende (black circles), wurtzite (red squares), or mixed-phase (blue triangles) cores. (f) Right to left: PL spectra after postsynthesis annealing of a CdSe/ZnSe core/shell product (wurtzite, 5 ML ZnSe), 200–310 °C. (g) X-ray diffraction patterns for same CdSe/ZnSe under different pressures. Rock salt (200) reflection indicated by asterisk. CdSe and ZnSe wurtzite reference patterns are green and red, respectively.

with a Cd-rich core.<sup>10</sup> Although not definitive, spectral data point to the latter. After addition of 12 ML equivalents of Zn and Se precursors, the calculated composition for the shown gQD is  $\text{Zn}_{0.95}\text{Cd}_{0.05}\text{Se}$ , and energy-dispersive X-ray spectroscopy (EDX) analysis confirms  $<10\%$  Cd metal content (Figure S1). Taking into account the known optical bowing parameter for the composition-dependent alloy bandgap,<sup>10</sup> the expected PL wavelength for this composition is 486 nm. The observed PL is  $\sim 525$  nm, suggesting that the product is not a fully homogeneous alloy but likely yet maintains a Cd-rich (possibly Zn-free) core.

In addition to SILAR anneal time, we assessed the impact of the CdSe core on whether core/shell or alloy formation prevails. Specifically, we repeated the short- and long-cycle SILAR reactions at 240 °C using wurtzite (hexagonal) and mixed-crystallographic-phase CdSe cores, rather than zinc blende (cubic) cores. Results for wurtzite-core reactions were similar to the above zinc-blende-core reactions, whereas mixed-phase-core reactions were stable to alloying for either long or short anneal times (Figure 2e), thereby denying a simple correlation between core crystal structure and the fate of



adatom addition. Other unknown factors (e.g., surface-<sup>8a</sup> or ligand-mediated processes,<sup>8b</sup> see Supporting Information) likely play key roles. Yet, in all cases, product crystal structures replicated those of the cores (Figure S2). For alloys, this suggests that cation substitution proceeds without lattice rearrangement. (Zinc blende products are  $\sim$ tetradedral,<sup>8a</sup> and wurtzite are more symmetric; see Figure 2a,c insets.)

To evaluate the stability of CdSe/ZnSe core/shell QDs to alloying postsynthesis, we annealed the products at high temperature (310 °C) and exposed them to high pressure (10.7 GPa). Annealing does not cause appreciable alloying (minimal PL blue-shifting, Figure 2f); whereas, under high pressure, the core and shell behave independently. Namely, consistent with literature,<sup>11</sup> the wurtzite CdSe core transforms to the rock salt crystal structure above  $\sim$ 5.6 GPa and then to  $\sim$ zinc blende upon return to 0 GPa (Figures 2g and S3). As expected for ZnSe (phase-transition pressure  $\approx$  13 GPa<sup>12</sup>), the shell is unaffected by our experiment ( $\sim$ 10 GPa). The postsynthesis integrity of core/shell CdSe/ZnSe further supports the hypothesis that surface-related processes during shelling are key to effecting shell vs alloy formation (see extended discussion, Supporting Information).

In contrast with CdSe/ZnSe QDs, the key challenge to ZnSe/CdS core/(thick)shell synthesis is to avoid Cd exchanging for Zn. Almost complete cation exchange has been shown for specific experimental conditions, i.e., high temperature (220 °C) and excess Cd,<sup>13</sup> and is supported by the more favorable Cd–Se compared to Zn–Se bond energy (310 vs 136 kJ/mol).<sup>14</sup> SILAR growth does not entail using excess Cd, and the inclusion of a S precursor means that Cd–S bond formation would compete with Zn–Se bond breaking/Cd–Se bond making. Thus, we did not a priori expect cation exchange to interfere with shell growth. After all, ZnSe/CdS core/(thin)shell QD synthesis had been reported previously.<sup>15</sup>

However, optical and elemental analysis data suggest that cation exchange is active in the ZnSe/CdS system. The large redshift in absorption and PL after addition of a single CdS ML (Figure 3a,b,  $>130$  nm, 240 °C SILAR) is inconsistent with

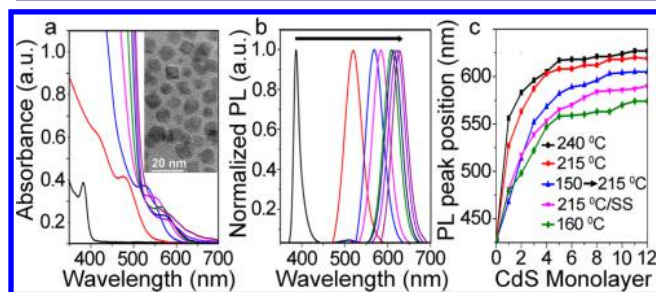


**Figure 3.** (a) Absorption (inset: TEM) and (b) PL spectra for ZnSe core (black trace) and after CdS shelling (red trace: 1 ML, then even MLs 2–12). (c) Summary of PL progression with CdS-shell ML for different shelling temperatures. Zn/Se ratio (2.3 nm radius core) = 0.6 (240 °C), 0.6 (215 °C), 0.7 (2 ML at 150 °C then 215 °C to 12 ML), 1.0 (215 °C, SS precursor), and 0.8 (160 °C).

calculations considering type II electronic structure alone. The final PL peak position (627 nm) is also red-shifted compared to theory, which requires a bandgap of  $2.1 \pm 0.05$  eV (577–605 nm) for an ideal core/(thick) shell product. Elemental analysis reveals a Zn/Se ratio of 0.4, rather than the 1:1 of an intact ZnSe core. We surmise that the core transforms to either a ZnSe/CdSe core/shell (3.1 nm ZnSe reduced to 2.3 nm with

formation of  $\sim$ 0.4 nm CdSe shell by cation exchange) or an alloy of composition  $\text{Zn}_{0.4}\text{Cd}_{0.6}\text{Se}$ . Thus, cation exchange causes composition redshifting that outpaces electronic-structure effects.

We modified SILAR growth to avoid cation exchange: lower temperatures or use of a single-source (SS) precursor (cadmium diethyldithiocarbamate). Lower temperatures limit cation exchange as indicated by spectral-shift and elemental analysis data (Figure 3c). However, PL quantum yields are reduced ( $<10\%$  vs  $>40\%$ , Supporting Information). A SS precursor eliminates Zn–Cd exchange, but optical properties suffer and the particle shape is asymmetric (rod-like, Figure S4).

Finally, CdSe/ZnSe and ZnSe/CdS gQDs were assessed for single-dot optical properties: blinking and relative biexciton emission efficiency as determined by second-order photon-correlation ( $g^{(2)}$ ) experiments (Supporting Information).<sup>16</sup> Individual CdSe/ZnSe gQDs exhibit PL intensity fluctuation, but rarely blink all the way off (Figure 4a, on-time fractions =

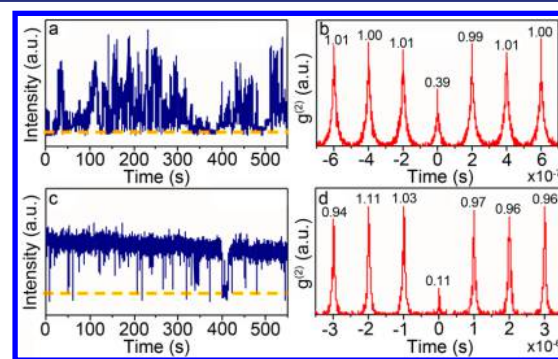


**Figure 4.** (a) Representative PL time trace for a CdSe/ZnSe gQD and (b) corresponding  $g^{(2)}$  trace (obtained for average per-dot carrier population  $< 0.2$ ; see Supporting Information). (c and d) Same for a ZnSe/CdS gQD. Dashed orange line in a and c is detection limit (below which gQD is off state).

0.4–0.8 and Figure S5). The large fluctuations between bright and less-intense gray states are the subject of further investigation, but may result from severe QD charging. In contrast to conventional QDs, charged gQDs are emissive (rather than dark) as a result of suppressed AR, where the efficiency of the charged-state emission depends on the extent of AR suppression<sup>17a</sup> and/or the degree of charging.<sup>17b</sup> Also indicative of reduced AR efficiency, this system is characterized by high  $g^{(2)}$  values (here  $\sim 0.4$ , Figure 4b), as anticipated for the combination of a quasi-type II electronic structure and thick-shell.

ZnSe/CdS gQDs grown at high temperature exhibit strongly suppressed shell-ML-dependent blinking, with the fraction of nonblinking gQDs approaching 60% for long interrogation times (Figures 4c and S6), though  $g^{(2)}$  values are unremarkable (Figure 4d). In contrast, other ZnSe/CdS QDs blink and rapidly photobleach. Thus, high-temperature growth paired with partial cation exchange substantially improves optical performance in this system.

We have shown two new examples of blinking/AR-suppressed QDs based on the gQD core/shell motif and type II electronic structure. Through careful control of shelling conditions, competing processes of alloying or cation exchange can be minimized or tuned for optimal performance.

## ■ ASSOCIATED CONTENT

### ■ Supporting Information

Experimental details, expanded discussion, and figures. This material is available free of charge via the Internet at <http://pubs.acs.org>.

## ■ AUTHOR INFORMATION

### Corresponding Author

\*jenn@lanl.gov

### Notes

The authors declare no competing financial interest.

## ■ ACKNOWLEDGMENTS

Funding from a Division of Materials Science and Engineering, Office of Basic Energy Sciences (OBES), Office of Science, U.S. Department of Energy (DOE) grant (2009LANL1096). Work performed largely at CINT, a DOE/OBES Nanoscale Science Research Center & User Facility. We thank D. Williams for obtaining XRDs.

## ■ REFERENCES

- (1) Talapin, D. V.; Lee, J.-S.; Kovalenko, M. V.; Shevchenko, E. V. *Chem. Rev.* **2010**, *110*, 389.
- (2) Hollingsworth, J. A.; Klimov, V. I. In *Semiconductor and Metal Nanocrystals: Synthesis, Electronic and Optical Properties*; Klimov, V. I., Ed.; Marcel Dekker: New York, 2003; pp 1–64.
- (3) (a) Chen, Y.; Vela, J.; Htoon, H.; Casson, J. L.; Werder, D. J.; Bussian, D. A.; Klimov, V. I.; Hollingsworth, J. A. *J. Am. Chem. Soc.* **2008**, *130*, 5026. (b) Mahler, B.; Spinicelli, P.; Buil, S.; Quélin, X.; Hermier, J. P.; Dubertret, B. *Nat. Mater.* **2008**, *7*, 659. (c) Dennis, A. M.; Mangum, B. D.; Piryatinski, A.; Park, Y.-S.; Hannah, D. C.; Casson, J. L.; Williams, D. J.; Schaller, R. D.; Htoon, H.; Hollingsworth, J. A. *Nano Lett.* **2012**, *12*, 5545. (d) Wang, X.; Ren, X.; Kahen, K.; Hahn, M. A.; Rajeswaran; Maccagnano-Zacher, S.; Silcox, J.; Cragg, G. E.; Efros, A. E.; D. Krauss, T. D. *Nature* **2009**, *459*, 686.
- (4) Pal, B. N.; Ghosh, Y.; Brovelli, S.; Laocharoensuk, R.; Klimov, V.; Hollingsworth, J. A.; Htoon, H. *Nano Lett.* **2012**, *12*, 331.
- (5) (a) Klimov, V. I.; Mikhailovsky, A. A.; Xu, S.; Malko, A.; Hollingsworth, J. A.; Leatherdale, C. A.; Eisler, H.-J.; Bawendi, M. G. *Science* **2000**, *290*, 314. (b) Caruge, J.-M.; Chan, Y.; Sundar, V.; Eisler, H. J.; Bawendi, M. G. *Phys. Rev. B* **2004**, *70*, 085316. (c) Dang, C.; Lee, J.; Breen, C.; Steckel, J. S.; Coe-Sullivan, S.; Nurmikko, A. *Nat. Nanotechnol.* **2012**, *7*, 335.
- (6) (a) Cui, J.; Beyler, A. P.; Bischof, T. S.; Wilson, M. W. B.; Bawendi, M. G. *Chem. Soc. Rev.* **2014**, *43*, 1287. (b) Galland, C.; Ghosh, Y.; Steinbrück, A.; Sykora, M.; Hollingsworth, J. A.; Klimov, V. I.; Htoon, H. *Nature* **2011**, *479*, 203.
- (7) (a) Li, J. J.; Wang, Y. A.; Guo, W. Z.; Keay, J. C.; Mishima, T. D.; Johnson, M. B.; Peng, X. G. *J. Am. Chem. Soc.* **2003**, *125*, 12567. (b) Xie, R. G.; Kolb, U.; Li, J. X.; Basche, T.; Mews, A. *J. Am. Chem. Soc.* **2005**, *127*, 7480. (c) van Embden, J.; Jasieniak, J.; Mulvaney, P. *J. Am. Chem. Soc.* **2009**, *131*, 14299. (d) Greytak, A. B.; Allen, P. M.; Liu, W.; Jing, Z.; Young, E. R.; Popović, Z.; Walker, B. J.; Nocera, D. G.; Bawendi, M. G. *Chem. Sci.* **2012**, *3*, 2028.
- (8) (a) Mahler, B.; Lequeux, N.; Dubertret, B. *J. Am. Chem. Soc.* **2010**, *132*, 953. (b) Ghosh, Y.; Mangum, B. D.; Casson, J. L.; Williams, D. J.; Htoon, H.; Hollingsworth, J. A. *J. Am. Chem. Soc.* **2012**, *134*, 9634.
- (9) (a) Reiss, P.; Bleuse, J.; Pron, A. *Nano Lett.* **2002**, *2*, 781. (b) Lee, Y.-J.; Kim, T.-G.; Sung, Y.-M. *Nanotechnology* **2006**, *17*, 3539.
- (10) Zhong, Z.; Han, M.; Dong, Z.; White, T. J.; Knoll, W. *J. Am. Chem. Soc.* **2003**, *125*, 8589.
- (11) Alivisatos, A. P. *J. Phys. Chem.* **1996**, *100*, 13226.
- (12) Köfferlein, M.; Karzel, H.; Potzel, W.; Schiessl, W.; Steiner, M.; Kalvius, G. M.; Mitchell, D. W.; Das, T. P. *Hyperfine Interact.* **1994**, *93*, 1505.
- (13) Zhong, X.; Feng, Y.; Zhang, Y.; Gu, Z.; Zou, L. *Nanotechnology* **2007**, *18*, 385606.
- (14) Dean, J. A., Ed. *Lange's Handbook of Chemistry*, 15th ed.; McGraw-Hill: New York, 1999.
- (15) Nemchinov, A.; Kirsanova, M.; Hewa-Kasakarage, N. N.; Zamkov, M. *J. Phys. Chem. C* **2008**, *112*, 9301.
- (16) (a) Park, Y.-S.; Malko, A. V.; Vela, J.; Chen, Y.; Ghosh, Y.; García-Santamaría, F.; Hollingsworth, J. A.; Klimov, V. I.; Htoon, H. *Phys. Rev. Lett.* **2011**, *106*, 187401–1–4. (b) Mangum, B. D.; Ghosh, Y.; Hollingsworth, J. A.; Htoon, H. *Opt. Express* **2013**, *21*, 7419.
- (17) (a) Spinicelli, P.; Buil, S.; Quélin, X.; Mahler, B.; Dubertret, B.; Hermier, J.-P. *Phys. Rev. Lett.* **2009**, *102*, 136801. (b) Galland, C.; Ghosh, Y.; Steinbrück, A.; Hollingsworth, J. A.; Htoon, H.; Klimov, V. I. *Nat. Commun.* **2012**, *3*, 908.